

Modeling the Solvent Sphere: Mechanism of the Shilov Reaction

Per E. M. Siegbahn*[†] and Robert H. Crabtree[‡]

Contribution from the Department of Physics, University of Stockholm, Box 6730, S-113 85 Stockholm, Sweden, and Chemistry Department, Yale University, 225 Prospect Street, New Haven, Connecticut 06511-8118

Received December 13, 1995. Revised Manuscript Received March 1, 1996[Ⓞ]

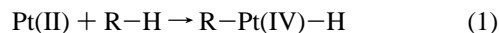
Abstract: Quantum chemical studies suggest that the Shilov reaction, the activation of alkane CH bonds by Pt salts in aqueous acid solution, goes via transfer of a hydrogen atom from a methane σ complex to a neighboring Cl ligand in what is best described as a σ bond metathesis. This avoids the formation of Pt(IV) and is quite similar to the mechanism proposed by Shilov himself. The hydrogen atom being transferred is not very protonic which is best seen by the fact that the transition state is not stabilized by additional water molecules in the bond breaking region, which would be expected to hydrogen bond to any protonic hydrogen. The calculated activation energy, with contributions from temperature and long-range dielectric effects, is in very good agreement with the experimental estimate. An alternative oxidative addition/reductive elimination sequence was found to be competitive for Pt. For Pd, the transition state energy for this pathway is much higher than for σ bond metathesis, and oxidative addition can therefore be disregarded. Although a σ bond metathesis mechanism seems more likely for Shilov chemistry with Pt, an oxidative addition/reductive elimination sequence cannot be safely excluded in the Pt case. The second coordination sphere of the solvent is found to play an important role in the Shilov reaction, both as ultimate proton acceptor from the methane and also in the energetics of methane binding; the latter directly contributes to the overall activation energy. The presence of only a few waters in the computational model allows these effects to be studied. The origin of the unusual preferential attack on primary versus secondary CH bonds in the system has been traced to the higher polarity of the *n*-alkyl versus the isoalkyl bond formed in the σ bond metathesis step.

Introduction

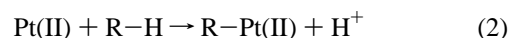
The Shilov reaction,^{1,2} alkane oxidation using soluble platinum salts, holds a central place in alkane activation chemistry.^{1–3} It was the first in a series of new alkane reactions that were discovered in the period 1970–85.³ The work developed from the results of Garnett and Hodges,⁴ who found that $[\text{PtCl}_4]^{2-}$ ion dissolved in an aqueous deuterated acid medium is capable of effecting H/D isotope exchange in arenes. Shilov and co-workers looked at essentially the same system, but with alkanes as substrates. This was an important and nonobvious experiment, because at that time, alkanes were considered inert to all reagents except metal surfaces, powerful oxidants like permanganate, and certain reactive radicals. The alkane is indeed deuterated under these conditions, and the selectivity pattern (primary C–H > secondary C–H > tertiary C–H)^{1b} was very unexpected because both radical and electrophilic reagents normally give selective attack at tertiary CH bonds. In a later variant of the reaction,^{1c} $[\text{PtCl}_6]^{2-}$ ion was used as a primary oxidant with the result that the alkane is chlorinated and hydroxylated; the selectivity remains essentially that of the Pt(II) catalyst (primary C–H > secondary C–H > tertiary C–H) however, and not that of radical or electrophilic chlorination. The results were so surprising that some observers looked for alternative explanations of the data. One early concern was that metallic platinum in colloidal form might be the active

catalyst, for example. By the early 1980s, however, this and other objections had been completely overcome, and interest shifted to discovering the detailed mechanism.¹ Recent work in this area has been carried out by Labinger and Bercaw⁵ and by Horvath.⁶

There are several puzzles associated with Shilov chemistry, which still remain unexplained. The first is simply that the system operates in aqueous solution, where one would expect that the alkane would not be able to compete with water for binding to the metal. The selectivity is remarkable; for example, the primary CH₃ group of both ethanol⁵ and propane¹ turns out to be more reactive than the CH₂ groups, which are normally much more reactive; even methane itself is reactive. The C–H bond selectivity resembles that of oxidative addition, but the oxidative addition pathway



seems for many reasons unlikely, in particular for the palladium analogue. Shilov proposed^{1,2} that the reaction starts out as an oxidative addition but that a proton is lost during the process (eq 2). In some cases, the R–Pt(II) fragment was trapped with



certain ligands and the resulting alkyl complex could be detected

(5) (a) Labinger, J. A.; Bercaw, J. A.; Luinstra, G. A.; Lyon, D. K.; Herring, A. M. In *Natural Gas Conversion II*; Curry-Hyde, H. E., Howe, R. F., Eds.; Elsevier: New York, 1994; p 515. (b) Labinger, J. A.; Herring, A. M.; Lyon, D. K.; Luinstra, G. A.; Bercaw, J. A. *Organometallics* **1993**, *12*, 895. (c) Luinstra, G. A.; Labinger, J. A.; Bercaw, J. A. *J. Am. Chem. Soc.* **1993**, *115*, 3004. (d) Luinstra, G. A.; Wang, L.; Stahl, S. S.; Labinger, J. A.; Bercaw, J. A. *Organometallics* **1994**, *13*, 755.

(6) Horvath, I. T.; Cook, R. A.; Millar, J. M.; Kiss, G. *Organometallics* **1993**, *12*, 8.

[†] University of Stockholm.

[‡] Yale University.

[Ⓞ] Abstract published in *Advance ACS Abstracts*, April 15, 1996.

(1) Shilov, A. E. *Activation of Saturated Hydrocarbons by Transition Metal Complexes*; D. Riedel: Dordrecht, The Netherlands, 1984; (b) p 152; (c) p 163; (d) pp 172–178; (e) p 148; (f) p 178.

(2) Shilov, A. E. In *Activation and Functionalization of Alkanes*; Hill, C. L., Ed.; Wiley: New York, 1984.

(3) Crabtree, R. H. *Chem. Rev.* **1985**, *85*, 245; **1995**, *95*, 987.

(4) Garnett, J. L.; Hodges, R. J. *J. Am. Chem. Soc.* **1967**, *89*, 4546.

(R = Me) or isolated and characterized (R = 2-naphthyl).¹⁴ The Shilov reaction has been extended to other metals, in the early period by Rudakov⁷ and recently, in a more detailed way, to Pd(II)⁸ and to Hg(II).⁹

Chemical reactions in aqueous solutions currently constitute an important and very active research area. Experimental information concerning the role of the solvent water molecules for the reactions is still very sparse. This is therefore an area where theoretical model calculations are particularly suitable in helping to provide increased understanding. However, the modeling of these reactions can be quite difficult. For reactions involving transition metal complexes there are four different types of interactions involving water molecules which affect chemical reactions. First, there are the water molecules that bind directly to the metal and therefore strongly influence the electronic and geometric structure of the metal complex. Second, there are the water molecules, sometimes from the second coordination sphere, that participate directly in the reaction through proton transfer, for example. These interactions are often the most difficult to model accurately. To stabilize the charges involved in a proton transfer, several water molecules might be needed. Third, there are the water molecules that hydrogen bond to the ligands of the metal complex. These water molecules may also require an explicit treatment in the computational model. Fourth, there are the water molecules that only contribute through the long-range polarizability. This dielectric effect can also be quite important for stabilizing charges that can appear in the reaction. The Shilov reaction is an interesting case where enough is known experimentally to allow an adequate test of the molecular models. Even though in principle many aspects of the aqueous solvent should ideally be considered, the present paper will show that outer sphere effects can sometimes be modeled by including only a modest number of water molecules in the computation. Since some of the key mechanistic details of the Shilov reaction still are lacking, another purpose of the present study is to provide some of this information. A detailed understanding of the Shilov reaction should help understanding other important reactions occurring in water, such as the Wacker process, in which the solvent water molecules are also directly involved in the reaction steps. The Wacker process has been studied in two recent papers, and many problems of fundamental importance have been identified.^{10,11} For example, the nucleophilic addition step is much more complicated than just a simple addition of an OH⁻, but requires the involvement of several water molecules. The O–H bond breaking step has also turned out to be quite difficult to model accurately. Work in progress uses more refined models to study these steps of the Wacker process.¹²

The present model calculations on the Shilov reaction for methane use the MCl₂(H₂O)₂ complexes as models for the active metal complexes, where the metal M is either palladium or platinum. Although the *trans*-dichloride is the species actually observed, calculations were also performed for the *cis*-form, where two different C–H dissociation pathways can be followed involving H dissociation both to a chloride and to a water ligand.

For the *trans*-species the water pathway is not relevant. Temperature and dielectric medium effects were also evaluated. Finally, in order to investigate the selectivity pattern for the C–H activation (see above), C–H bond breaking in propane for either a central C–H bond or a terminal C–H bond was studied. Most of the calculations were done at the hybrid DFT (density functional theory) level, but some energies were also evaluated using recently parametrized *ab initio* methods.

Computational Details

Most of the present calculations have been performed using an empirically parametrized (DFT) method, hereafter termed B3LYP. The B3LYP functional can be written as

$$E^{\text{B3LYP}} = (1 - A)F_x^{\text{Slater}} + AF_x^{\text{HF}} + BF_x^{\text{Becke}} + CF_c^{\text{LYP}} + (1 - C)F_c^{\text{VWN}}$$

where F_x^{Slater} is the Slater exchange, F_x^{HF} is the Hartree–Fock exchange, F_x^{Becke} is the exchange functional of Becke,¹³ F_c^{LYP} is the correlation functional of Lee, Yang, and Parr,¹⁴ and F_c^{VWN} is the correlation functional of Vosko, Wilk, and Nusair.¹⁵ A , B , and C are the coefficients determined by Becke¹³ using a fit to experimental heats of formation for a common benchmark test¹⁶ consisting of 55 first- and second-row molecules. However, it should be noted that Becke did not use F_c^{LYP} in the expression above when the coefficients were determined, but used the correlation functional of Perdew and Wang instead.¹⁷ The introduction of gradient corrections, Hartree–Fock exchange, and empirical parameters has made this type of hybrid DFT approach highly competitive in accuracy with the most accurate standard quantum chemical methods. For large systems it is very much faster than more accurate standard correlation methods. The B3LYP calculations were carried out using the GAUSSIAN92/DFT package.¹⁸

For some of the present palladium systems comparative calculations were performed using the recently developed PCI-80 scheme.^{19,20} This parametrized scheme is based on calculations performed using the modified coupled pair functional (MCPF) method,²¹ which is a standard quantum chemical, size-consistent, single reference state method. The zeroth-order wave functions were determined at the SCF level. All valence electrons were correlated including the 4d and 5s electrons on the palladium atom. If standard double ζ plus polarization (DZP) basis sets are used, it has been shown that about 80% of the correlation effects on bond strengths are obtained irrespective of the system studied. A good estimate of a bond strength is thus obtained by simply adding 20% of the correlation effects, and this is what is done in the PCI-80 scheme.¹⁹ The parameter 80 is thus an empirical parameter, which is not fitted but still chosen to give agreement with experiment for a similar benchmark test as the one used for the B3LYP method. There are thus clear similarities between these methods in this respect. The use of a single scaling parameter for the entire periodic table is the key feature of the PCI-80 scheme. Other scaling schemes exist, such

(13) Becke, A. D. *Phys. Rev.* **1988**, A38, 3098. Becke, A. D. *J. Chem. Phys.* **1993**, 98, 1372. Becke, A. D. *J. Chem. Phys.* **1993**, 98, 5648.

(14) Lee, C.; Yang, W.; Parr, R. G. *Phys. Rev.* **1988**, B37, 785.

(15) Vosko, S. H.; Wilk, L.; Nusair, M. *Can. J. Phys.* **1980**, 58, 1200.

(16) Pople, J. A.; Head-Gordon, M.; Fox, D. J.; Raghavachari, K.; Curtiss, L. A. *J. Chem. Phys.* **1989**, 90, 5622.

(17) Perdew, J. P.; Wang, Y. *Phys. Rev. B* **1992**, 45, 13244. Perdew, J. P. In *Electronic Structure of Solids*; Ziesche, P., Eischrig, H., Eds.; Akademie Verlag: Berlin, 1991. Perdew, J. P.; Chevary, J. A.; Vosko, S. H.; Jackson, K. A.; Pederson, M. R.; Singh, D. J.; Fiolhais, C. *Phys. Rev. B* **1992**, 46, 6671.

(18) GAUSSIAN 92/DFT, Revision G.1: M. J. Frisch, G. W. Trucks, M. Head-Gordon, P. M. W. Gill, M. W. Wong, J. B. Foresman, B. G. Johnson, H. B. Schlegel, M. A. Robb, E. S. Replogle, R. Gomperts, J. L. Andres, K. Raghavachari, J. S. Binkley, C. Gonzales, R. L. Martin, D. J. Fox, D. J. Defrees, J. Baker, J. J. P. Stewart, and J. A. Pople, Gaussian, Inc. Pittsburgh, PA, 1993.

(19) Siegbahn, P. E. M.; Blomberg, M. R. A.; Svensson, M. *Chem. Phys. Lett.* **1994**, 223, 35.

(20) Siegbahn, P. E. M.; Svensson, M.; Boussard, P. J. E. *J. Chem. Phys.* **1995**, 102, 5377.

(21) Chong, D. P.; Langhoff, S. R. *J. Chem. Phys.* **1986**, 84, 5606.

(7) Rudakov, E. S.; Lutsyk, A. I. *Neftekhimia* **1980**, 20, 163. See also ref 1, pp 70–73.

(8) Gretz, E.; Oliver, T. F.; Sen, A. *J. Am. Chem. Soc.* **1987**, 109, 8109. Sen, A. *Platinum Met. Rev.* **1991**, 35, 126. Kao, L. C.; Hutson, A. C.; Sen, A. *J. Am. Chem. Soc.* **1991**, 113, 700. Sen, A.; Benvenuto, M. A.; Lin, M.; Basicke, N. *J. Am. Chem. Soc.* **1994**, 116, 998.

(9) Periana, R. A.; Taube, D. J.; Evtitt, E. R.; Loeffler, D. G.; Wentreck, P. R.; Voss, G.; Matsuda, T. *Science* **1993**, 259, 340.

(10) Siegbahn, P. E. M. *Struct. Chem.* **1995**, 6, 271.

(11) Siegbahn, P. E. M. *J. Am. Chem. Soc.* **1995**, 117, 5409.

(12) Siegbahn, P. E. M.; Crabtree, R. H. To be published.

as those due to Truhlar et al.²² In those schemes different parameters are used for different systems. In the PCI-80 calculations relativistic effects were added using perturbation theory for the mass-velocity and Darwin terms.²³ The PCI-80 calculations were performed using the STOCKHOLM set of programs.²⁴

Essentially the same standard DZP basis sets were used for both the B3LYP and the PCI-80 calculations. For first-row atoms the primitive (9s, 5p) basis of Huzinaga²⁵ was used, contracted according to the generalized contraction scheme to [3s, 2p], and one d function was added. For hydrogen the primitive (5s) basis from ref 24 was used in the PCI-80 calculations, augmented with one p function and contracted to [3s, 1p]. For the B3LYP calculations a primitive (4s, 1p) basis contracted to [2s, 1p] was used instead. In the PCI-80 calculations an all-electron description was used for the palladium atom using the Huzinaga primitive basis²⁶ extended by adding one diffuse d function, two p functions in the 5p region, and three f functions, yielding a (17s, 13p, 9d, 3f) primitive basis. The core orbitals were totally contracted except for the 4s and 4p orbitals which have to be described by at least two functions each to properly reproduce the relativistic effects. The 5s and 5p orbitals were described by a double ζ contraction and the 4d by a triple ζ contraction. The f functions were contracted to one function giving a [7s, 6p, 4d, 1f] contracted basis. For the B3LYP calculations, on the other hand, the relativistic effective core potentials (RECPs) according to Hay and Wadt²⁷ were used for palladium and platinum. In these RECPs, the valence orbitals are described by a double ζ basis except for the d orbital which is described by a triple ζ basis. No f functions were used. In the PCI-80 calculations, the polarization functions were removed on the atoms not directly involved in the bond for which the bond strength is evaluated. This saves considerable computer time, and the experience using this procedure is quite good.

All the geometries of the present study have been optimized at the B3LYP level using the above basis sets without polarization functions. All degrees of freedom were optimized. Zero-point vibrational effects were added on the basis of B3LYP calculations for the reactions between $\text{PdCl}_2(\text{H}_2\text{O})_2$ and methane. From the computed Hessians temperature dependent enthalpy effects and entropy contributions were also obtained following procedures from standard textbooks.²⁸ The temperature used was 298.15 K.

The simplest way to obtain an estimate of long-range dielectric effects is to use the Onsager model.^{29,30} In this model, a spherical cavity is placed around the molecule and the solvent is described as a dielectric medium. The dipolar energy contribution of the solvation energy is then given by

$$E = \frac{\epsilon - 1}{2\epsilon + 1} \frac{\mu^2}{R^3}$$

where R is the cavity radius and ϵ is the dielectric constant. These effects were obtained self-consistently using the SCRf (self-consistent reaction field) method as implemented in the GAUSSIAN92/DFT program. The dielectric constant of water was taken to be 80.4. The cavity radii were obtained following the standard procedure in the program. The volume inside a contour of 0.001 electron/bohr³ density was first determined. The radius of the spherical cavity is then taken to be 0.5 Å larger than the radius corresponding to this volume.

(22) Brown, F. B.; Truhlar, D. G. *Chem. Phys. Lett.* **1985**, *117*, 307. Gordon, M. S.; Truhlar, D. G. *J. Am. Chem. Soc.* **1986**, *108*, 5412. Gordon, M. S.; Truhlar, D. G. *Int. J. Quantum Chem.* **1987**, *31*, 81. Gordon, M. S.; Nguyen, K. A.; Truhlar, D. G. *J. Phys. Chem.* **1989**, *93*, 7356.

(23) Martin, R. L. *J. Phys. Chem.* **1983**, *87*, 750. See also: Cowan, R. D.; Griffin, D. C. *J. Opt. Soc. Am.* **1976**, *66*, 1010.

(24) STOCKHOLM is a general purpose quantum chemical set of programs written by P. E. M. Siegbahn, M. R. A. Blomberg, L. G. M. Pettersson, B. O. Roos, and J. Almlöf.

(25) Huzinaga, S. *J. Chem. Phys.* **1965**, *42*, 1293.

(26) Huzinaga, S. *J. Chem. Phys.* **1977**, *66*, 4245.

(27) Hay, P. J.; Wadt, W. R. *J. Chem. Phys.* **1985**, *82*, 299.

(28) McQuarrie, D. A. *Statistical Thermodynamics*; Harper and Row: New York, 1973.

(29) Onsager, L. *Electr. Moments Liq.* **1936**, *58*, 1486.

(30) Wong, M. W.; Frisch, M. J.; Wiberg, K. B. *J. Am. Chem. Soc.* **1991**, *113*, 4776.

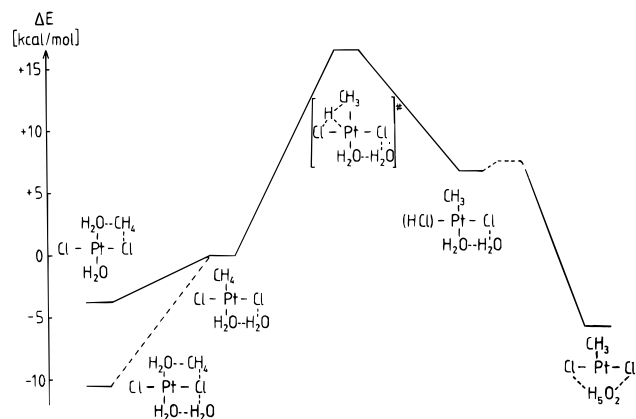


Figure 1. Free energies along the reaction pathway for the reaction between $\text{PtCl}_2(\text{H}_2\text{O})_2$ and methane. The energies include an estimate for long-range dielectric effects. At the bottom left the relative energy for the $[\text{PtCl}_2(\text{OH}_2)_2](\text{CH}_4)(\text{H}_2\text{O})$ complex compared to the $[\text{PtCl}_2(\text{OH}_2)_2](\text{CH}_4)(\text{H}_2\text{O})_2$ complex is also shown. The energies were obtained at the B3LYP level except for the $(\text{H}_5\text{O}_2)^+$ structure which was obtained at the PCI-80 level.

Results and Discussion

The discussion of the results from the model calculations on the Shilov reaction is divided into six subsections. Most of the discussion will focus on results for the reaction between methane and the $\text{PtCl}_2(\text{H}_2\text{O})_2$ *trans*-dichloride complex, but some results for the corresponding palladium complex and also for the *cis*-dichloride complex will also be mentioned. The free energies (298.15 K) obtained for selected points along the reaction pathway for the platinum *trans*-dichloride reaction are displayed in Figure 1. These energies include an estimate of long-range dielectric effects. In the first subsection the initial step of the Shilov reaction is discussed. This is the methane-water ligand exchange, for which two different models have been used. The critical C-H activation step is discussed in the second subsection and the final step of the reaction in the third. In the fourth subsection, the problem of primary versus secondary C-H bond activation is discussed for the case of the reaction with propane. Finally, in the fifth and sixth subsections, the alternative reaction pathway following an oxidative addition/reductive elimination mechanism is investigated.

a. Methane-Water Ligand Exchange. One of the main surprises in the Shilov reaction is that an alkane is able to replace a directly bound water ligand. If palladium is taken as an example, the metal-water bond strength for a *trans*-dichloride is about 30 kcal/mol (without zero-point vibrational effects) while the metal-methane bond strength is only about 10 kcal/mol. The bond strengths are about the same for platinum. It therefore appears as if it would require an activation energy of about 20 kcal/mol to attach methane directly to the metal. There are several obvious approximations in this reasoning, the main one being the neglect of the presence of the second coordination shell. If this shell is taken into account, a simple estimate leads to a quite different result. In the second coordination shell, methane is expected to have very weak binding to the complex since it lacks a dipole moment and the distance to the metal is quite large. A second sphere bond strength of only about 3 kcal/mol is therefore probably a reasonable estimate. Water on the other hand has a relatively large dipole moment and is therefore substantially bound in the second coordination shell. Calculations give a value of about 18 kcal/mol for the second sphere bond strength of water to a square planar $\text{PdCl}_2(\text{H}_2\text{O})_2$ complex.³¹ If these bond strengths are included in the model,

(31) Siegbahn, P. E. M.; Crabtree, R. H. *Mol. Phys.*, in press.

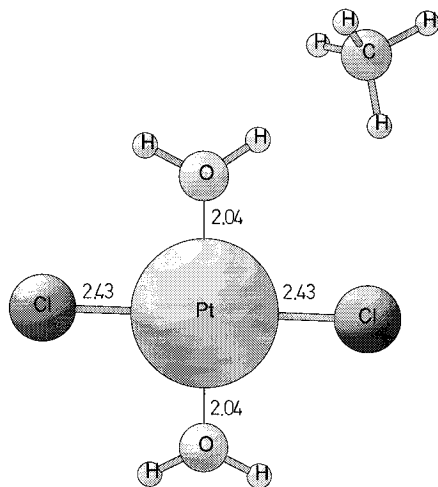


Figure 2. Structure of the $[\text{PtCl}_2(\text{OH})_2](\text{CH}_4)$ complex. The free energy difference compared to the structure in Figure 3 is -3.8 kcal/mol.

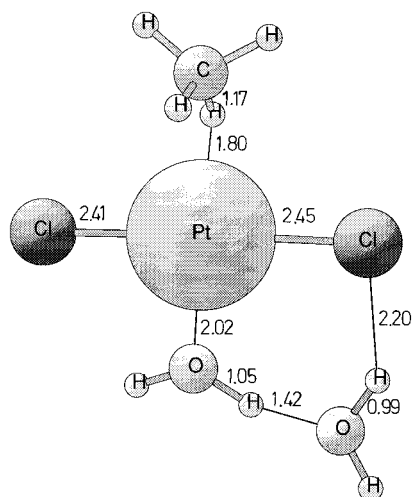


Figure 3. Structure of the $[\text{PtCl}_2(\text{OH})_2](\text{CH}_4)(\text{H}_2\text{O})$ complex.

the exchange of water and methane between the first and second coordination shells should cost only about 5 kcal/mol, an easily accessible energy. However, this model still contains several simplifications, such as the effect of the methane on the different metal–water bond strengths. It can be added that exchanging a chloride with a water molecule from the second coordination shell is too costly to improve the methane–water ligand exchange. At the present computational level the chloride–water exchange is endothermic by about 10 kcal/mol.

The simplest model which is able to describe methane–water exchange is given in eq 3 where we use square brackets to designate the inner sphere. The optimal geometry with methane



in the second coordination shell is shown in Figure 2, while the corresponding geometry with methane directly bound to the metal is shown in Figure 3. The energy difference between these two structures is quite small for platinum, only 3.8 kcal/mol in favor of the structure in Figure 2. This value is thus not far away from the second simple estimate given above. Since the dipole moment is higher for the structure of Figure 3, the effect of the dielectric medium, studied through an SCRF calculation, is to lower the energy difference still further to 1.6 kcal/mol. Zero-point vibrational effects and temperature effects lead to a final energy difference of 3.8 kcal/mol between these

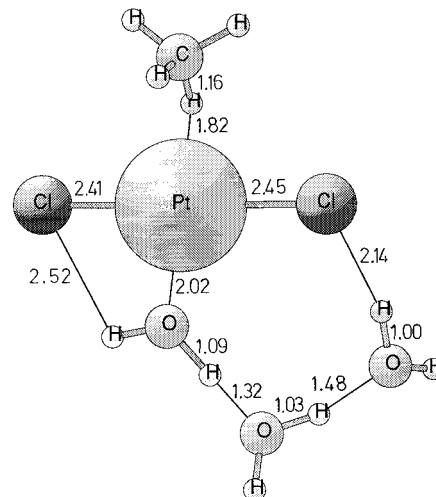


Figure 4. Structure of the $[\text{PtCl}_2(\text{OH})_2](\text{CH}_4)(\text{H}_2\text{O})_2$ complex. The free energy difference compared to the structure where methane is in the second coordination shell is $+10.5$ kcal/mol.

two structures. For palladium *trans*-dichloride the energy difference is very similar, 4.6 kcal/mol. The temperature effects consist of two components with opposite effects. The temperature dependent enthalpy effect stabilizes the methane complex of Figure 3 by 1.4 kcal/mol while the entropy effect destabilizes this structure by 3.6 kcal/mol. The latter effect can be rationalized by the higher degree of rigidity when methane is bound to the metal.

The above simple model is probably quite reasonable, but one striking feature casts some doubt on it. As seen in Figure 3, the water molecule in the second coordination shell does not take the position occupied by methane in Figure 2. Instead, when methane is attached to the metal, water swings around the Pt–Cl bond to bind on the other side via a hydrogen bond to the water ligand. In fact, this geometric change is quite important, on the order of 10–15 kcal/mol. It is clear that this geometry change requires that the new position for water is available and not already occupied by another water molecule. In the simple model used, this position may be too easily available since no additional solvent molecules are present. The model should therefore be improved by simply placing an additional water molecule in this position to prevent the geometric change of Figure 3 from occurring. Some calculations were therefore performed on a model with one additional water molecule. The position close to methane is again very hydrophobic, and water still does not want to occupy this position. When water swings around the Pt–Cl bond, water has to squeeze into the site between the water originally in this position and the chloride ligand. This leads to the structure shown in Figure 4, with an energy difference of 10.5 kcal/mol compared to the corresponding calculation where methane is in the second coordination shell. It is clear that the result using this model still has some uncertainties. It should, for example, be added that the entropy gain by coordinating methane to the metal, as compared to the situation where methane is surrounded by water, is neglected since it is very difficult to obtain a reliable estimate for this quantity. However, no other tractable model appears substantially better than the ones used here.

The structures in Figures 2–4 contain some interesting features worth noting. First, the methane molecule is η^1 -coordinated to the metal with a rather short Pt–H bond distance of 1.80 Å and a long C–H distance of 1.17 Å. The second shortest Pt–H distance is 2.43 Å. For the corresponding Pd complex, methane is more nearly η^2 -coordinated with Pd–H distances of 1.95 and 2.29 Å. The most interesting aspect of

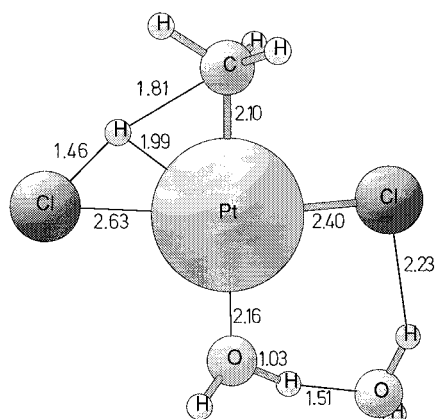
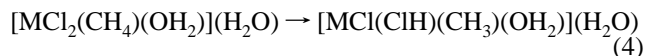


Figure 5. Structure of the C–H activation transition state for the reaction between methane and the $\text{PtCl}_2(\text{H}_2\text{O})_2$ complex following the σ bond metathesis pathway. The free energy difference compared to the structure in Figure 3 is +16.5 kcal/mol.

the structure in Figure 4 concerns the O–H distances. The O–H bonds in water molecules which are just hydrogen bonded are about 1.0 Å. A typical $\text{O}\cdots\text{H}$ hydrogen bond distance is in the range 1.6–1.8 Å. In Figure 2 there is one $\text{O}\cdots\text{H}$ bond distance with an intermediate length of 1.42 Å, and in Figure 4 there are two intermediate $\text{O}\cdots\text{H}$ bond distances of 1.32 and 1.48 Å. This shows that there is some tendency for Pt–OH covalent bonding in the direct platinum–water interaction and also some tendency for formation of a $(\text{H}_3\text{O}_2)^+\text{Cl}^-$ ionic complex in the outer sphere.

PCI-80 calculations were performed for the critical binding energy of methane to the metal center. These calculations were done for the $\text{PdCl}_2(\text{H}_2\text{O})(\text{CH}_4)$ *trans*-dichloride complex. The result was a bond strength of 15.2 kcal/mol compared to the B3LYP result of 12.1 kcal/mol. These energies do not contain zero-point, temperature, or dielectric effects. Since the PCI-80 scheme is known to slightly overestimate these bond strengths, the B3LYP result appears quite reasonable, perhaps being a few kilocalories per mole too small.

b. C–H Dissociation Step. The key part of the Shilov reaction is clearly the C–H activation step. Two different mechanisms have been suggested for this activation (see the Introduction). The first one is simply oxidative addition leading to a Pt(IV) complex (see subsections e and f). The second one, suggested by Shilov, is that a proton is lost during the activation step. The calculations on the present model systems, eq 4, lead



to a transition state with the structure shown in Figure 5. As seen in this figure there is a four-center transition state resembling that of σ bond metathesis. The hydrogen atom moves between methane and chlorine while retaining a short Pt–H distance. At the transition state the Pt–H distance is 1.99 Å. Since an HCl ligand is being formed, the Pt–Cl distance increases from 2.41 to 2.63 Å. The Pt–C distance shortens from 2.42 to 2.10 Å. A few minor effects can be noted for the nonactive water and chloride ligands. The second Pt–Cl bond and the Pt– H_2O bonds are strengthened somewhat as the first Pt–Cl bond is weakened. The second Pt–Cl distance goes from 2.45 to 2.40 Å and the Pt–O distance from 2.16 to 2.02 Å. There is also a slight increase of the distance between the water molecules from 1.42 to 1.51 Å, indicating somewhat less polarity in this region. The charges on the different atoms do not change significantly in this process. The hydrogen atom transferred has a charge of +0.23 at the transition state versus

a charge of +0.26 in the η^1 -coordinated form. The other hydrogen atoms on methane have charges in the range +0.19 to +0.22. As a consequence of these small charge changes, the dipole moment hardly changes at all from 3.21 to 2.74 D.

The energy at the transition state is 20.5 kcal/mol higher than for the methane complex of Figure 3. Since a C–H bond ($\text{H}-\text{CH}_3$) containing a large amount of zero-point vibration is broken and a bond ($\text{H}-\text{Cl}$) with much less zero-point vibration is formed, the net effect of zero-point vibration is to lower the transition state energy by 3.7 kcal/mol. Temperature effects lower the transition state still further by 1.4 kcal/mol to 15.4 kcal/mol. Long-range dielectric effects finally increase the transition state energy by 1.1 kcal/mol to a final value of 16.5 kcal/mol. It should be noted that the total activation energy of the Shilov reaction is the sum of this energy and the energy required to form the methane complex of Figure 4. From the results in the previous subsection the predicted total activation energy is thus the sum of 16.5 and 10.5 kcal/mol which is 27.0 kcal/mol. Experimentally, the activation energy has been measured for benzene (25.7 kcal/mol in H/D exchange and 25 kcal/mol in oxidation),¹ and since CH_4 reacts about 15 times slower, the activation energy should be close to 28 kcal/mol. The very good agreement between the calculated activation energy and the experimental estimate must be regarded as fortuitous to some extent considering the present model assumptions, but shows that the model used at least is quite reasonable. The energy difference between the methane complex and the transition state is almost identically the same for the palladium and platinum *trans*-dichlorides, differing only by 0.1 kcal/mol. The corresponding energy difference for the *cis*-dichloride of palladium is significantly higher than for the *trans*-dichloride, by 6.7 kcal/mol. This effect is attributed to the weaker Pd–Cl polarity in the *cis*-dichloride systems. A larger charge on the chloride helps in the abstraction of the hydrogen and also leads to a less directional character of the chloride bond.

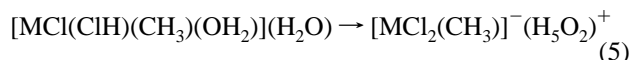
Since the water molecule in the second coordination shell is far away from the site of the C–H activation (see Figure 5), the importance of including it might be questioned. In fact it was only included to keep the system as much as possible the same from start to end of the entire reaction. However, for the *trans*-dichloride of palladium the calculations were repeated without this ligand. This had as expected a rather small effect, lowering the barrier by 2.2 kcal/mol. An attempt was also made to place a water molecule close to the hydrogen atom being transferred in order to see if this could stabilize the transition state. The result of this optimization was that the added water molecule moved away from this region with a considerable gain in energy. This calculation is perhaps the best illustration of the fact that the hydrogen atom transferred is not protonic. If it would have been protonic, the added water molecule should have stayed in the neighborhood and stabilized the protonic charge. The Mulliken charge on the transferred hydrogen atom does not indicate any protonic character either, being about the same as the ones for the hydrogen atoms in methane. It can be added that the possible hindrance for the hydrogen transfer from having water molecules in the neighborhood should be energetically very small, since the water molecules can easily move out of the way.

For the *cis*-dichloride an alternative reaction pathway was also investigated, in which the C–H bond dissociates toward the water ligand. In order to promote this transfer a prior step is introduced in which the two water molecules in the model form one OH^- ligand directly bound to the metal and one second sphere H_3O^+ group bound in between the chloride ligands. For

platinum *cis*-dichloride this step requires 12.8 kcal/mol (without zero-point and temperature effects). For palladium the energy requirement is very similar, 12.1 kcal/mol. From this point the C–H bond can now dissociate toward the OH ligand and form water. For platinum this point is 26.8 kcal/mol higher than the starting point with attached methane and water ligands. For palladium this energy is 28.2 kcal/mol. This means that for the palladium *cis*-dichloride this reaction pathway is unfavorable compared to the dissociation toward a chloride by only 1.1 kcal/mol. However, both barriers for the *cis*-dichloride are substantially higher than the one for the *trans*-dichloride, and a rearrangement from the *trans*- to the *cis*-dichloride in order to dissociate the C–H bond is therefore ruled out.

PCI-80 energies were evaluated for some of the structures discussed above. These benchmark test calculations were made at the outset, and the system was therefore the palladium *cis*-dichloride. For the energy barrier from the structure where methane is attached to the metal to the transition state for C–H dissociation toward a chloride, the discrepancy between the PCI-80 energy and the B3LYP energy is only 0.9 kcal/mol, so the energies obtained at the B3LYP level should be quite reliable for this type of pathway. This is important since this is the most plausible type of pathway. For the other pathway where the dissociation goes toward the water ligand, the discrepancy is larger. For the first step where the OH ligand and the H₃O⁺ group are formed the PCI-80 energy cost is 4.9 kcal/mol higher than the one at the B3LYP level. For the second step, leading to the transition state, the PCI-80 energy is also higher, now by 5.6 kcal/mol, than the B3LYP energy. This means that this pathway, which was already ruled out on the basis of the results at the B3LYP level, becomes even less likely on the basis of the PCI-80 results. It can be added that, in general, results both at the B3LYP level and at the PCI-80 level are found to give good agreement with available experiments.³² However, results such as some of the present ones show that this is not always the case and it is therefore important to continue to do calculations at different levels in order to get better estimates of the errors.

c. Final Part of the Reaction. The final part of the Shilov reaction considered here is a proton transfer from the HCl ligand to an outer sphere water:



From the σ bond metathesis transition state in Figure 5, this pathway goes via an intermediate which has a very shallow local energy minimum. This intermediate, shown in Figure 6, can be described as an HCl complex analogous to halocarbon complexes.³³ Apart from the HCl ligand, the structure of Figure 6 is quite similar to the one for the transition state in Figure 5. The Pt–C distance is slightly shorter, 2.04 Å compared to 2.10 Å, and the distance to the active chloride ligand is also slightly shorter, 2.58 Å compared to 2.63 Å, while the Pt–O distance is longer, 2.24 Å compared to 2.16 Å. The rest of the complex remains almost perfectly intact. The energy difference between the HCl complex in Figure 6 and the complex in Figure 3 is 10.2 kcal/mol in favor of the one in Figure 3. Adding zero-point vibrational and temperature effects leads to an energy difference of 7.6 kcal/mol. Long-range dielectric effects further decrease the energy difference to 6.7 kcal/mol. These energy differences are very similar for the corresponding palladium complex.

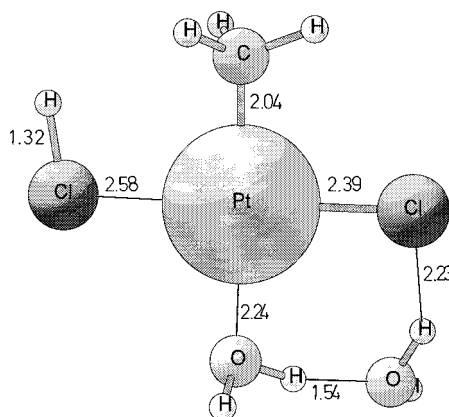


Figure 6. Structure of the $[\text{PtCl}(\text{ClH})(\text{CH}_3)(\text{OH}_2)](\text{H}_2\text{O})$ complex. The free energy difference compared to the structure in Figure 3 is +6.7 kcal/mol.

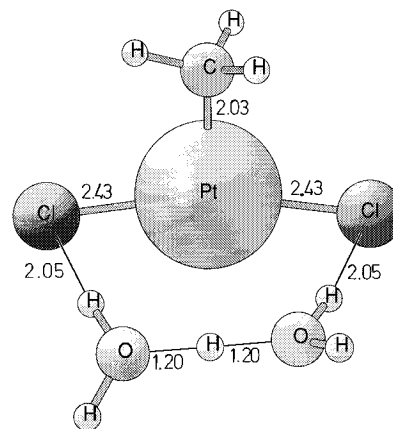


Figure 7. Structure of the $\text{PtCl}_2(\text{CH}_3)(\text{H}_5\text{O}_2)$ complex. The free energy difference compared to the structure in Figure 3 is –5.9 kcal/mol at the PCI-80 level.

The structure in Figure 6 goes over a very small energy barrier as the hydrogen swings over to the other side of the Pt–Cl bond. This energy barrier was not determined but must be small, at most a few kilocalories per mole, on the basis of the fact that it was very difficult to obtain geometry convergence to the structure in Figure 6. Even small deviations of the starting geometry lead to dissociation of the Cl–H bond, with the hydrogen moving toward the water ligand. A precise value of the energy barrier for breaking the Cl–H bond is furthermore without much significance for the present overall reaction as long as the barrier is small. It can be added that a determination of a transition state for a reaction with a very small barrier is computationally very difficult and the structure obtained will be very sensitive to the level of treatment. Passing the small barrier, the complex reorganizes to the quite symmetric structure shown in Figure 7. This structure contains an $(\text{H}_5\text{O}_2)^+$ ligand with two hydrogen bonds to the chlorides. The distances between the central proton and the two oxygens are quite short, only 1.20 Å. The ionic character of this complex is seen by the quite large dipole moment of 8.30 D compared to, for example, 2.74 D, at the transition state in Figure 5. The energy difference between the structure of Figure 7 and the one in Figure 3 is very small, only 0.8 kcal/mol in favor of the one in Figure 3. Zero-point vibrational and temperature effects lead to a reversal of stability favoring the structure in Figure 7 by 0.6 kcal/mol. However, a much more important effect is the long-range dielectric effect. Due to the large dipole moment for the structure in Figure 7, this structure is now favored by as much as 13.2 kcal/mol. An interesting aspect of the structure

(32) Blomberg, M. R. A.; Siegbahn, P. E. M.; Svensson, M. *J. Chem. Phys.*, in press.

(33) Kulawiec, R. J.; Crabtree, R. H. *Coord. Chem. Rev.* **1990**, 99, 89.

in Figure 7 is that the $(\text{H}_5\text{O}_2)^+$ group is in a plane which is essentially perpendicular to the plane defined by the other three ligands. The vacant site in the plane of this 3-coordinate T-shaped complex is stabilized by the *trans* effect of the methyl group.

For the $(\text{H}_5\text{O}_2)^+$ complex a significant difference between the B3LYP energy and the PCI-80 energy was found. For the corresponding palladium *trans*-dichloride complex the stability with respect to the methane structure shown in Figure 3 is 7.3 kcal/mol smaller at the PCI-80 level than at the B3LYP level. This is a rather important difference in the present context. With this 7.3 kcal/mol correction the $(\text{H}_5\text{O}_2)^+$ complex becomes less stable by 4.6 kcal/mol than the starting complex with methane in the second sphere (corresponding to the complex in Figure 4). This instability of the $(\text{H}_5\text{O}_2)^+$ complex is necessary in order to explain the experimental fact that this methyl complex is not observed experimentally.¹ Experimentally, only isotope exchange is observed.

Reversal of the steps described above, with a D^+ coming from the solvent, leads to isotope exchange in the methane. Shilov¹ noted that multiple H/D exchange occurs before substrate dissociation from the catalytic site. This may be a result of the stability of the methane complex, which is therefore able to undergo several CH dissociation steps before leaving the site. The chlorination/hydroxylation chemistry seen with $[\text{PtCl}_6]^{2-}$ as primary oxidant may result from inner sphere oxidation of the Pt(II)–Me species to the Pt(IV)–Me form, followed by nucleophilic displacement of platinum by attack of Cl^- or H_2O on the Pt(IV)–Me. We have not considered these steps in detail in this paper, however.

d. Primary versus Secondary C–H Bond Activation. One of the unusual features of the Shilov reaction is that primary C–H bonds are more easily activated than secondary C–H bonds. To see if this result could be reproduced by the present simple models, calculations were performed for C–H activation for a terminal and a central C–H bond of propane. To reduce the cost of the calculations, one of the water ligands (the one in the second coordination shell) was removed. This was shown (see subsection b) to have only a very small effect on the reaction energies. Ideally, the transition state for C–H bond breaking should then be compared for the activation of the two different C–H bonds. However, for the present reaction the point on the reaction pathway where the molecular HCl ligand is present (see Figure 6) is sufficiently close to the transition state that this point can be used for the comparison, following the Hammond postulate.³⁴ This simplifies the calculations considerably since a minimum is much more readily located than a transition state. The structure obtained for the *n*-propyl ligand is shown in Figure 8.

The first point of interest in the calculations concerns the strengths of the different C–H bonds in propane itself. At the B3LYP level these bond strengths are 97.6 kcal/mol for a terminal C–H bond and 94.0 kcal/mol for a central C–H bond. This difference of 3.6 kcal/mol is what normally makes the central C–H bond easier to activate. The corresponding values at the PCI-80 level are somewhat higher with values of 100.6 and 98.2 kcal/mol, respectively, which leads to a slightly smaller difference of 2.4 kcal/mol. Experimental values are 101.2 and 98.1 kcal/mol, respectively.³⁵

For the Pt–(HCl) *n*-propyl and isopropyl complexes the calculated energies favor the *n*-propyl complex by 1.4 kcal/mol at the B3LYP level. This means that the Pt– $\text{C}_3\text{H}_7(n)$ bond

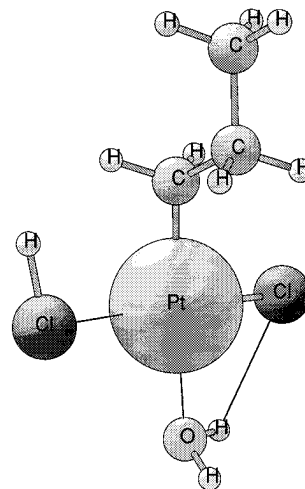


Figure 8. Structure of the $\text{PtCl}(\text{HCl})(\text{C}_3\text{H}_7)(\text{H}_2\text{O})$ complex, obtained after activation of a terminal C–H bond in propane.

is as much as 5.0 kcal/mol stronger than the Pt– $\text{C}_3\text{H}_7(\text{iso})$ bond. The results for the present model are thus in accord with experiments which show a higher tendency for primary than for secondary C–H activation. The origin of the stronger Pt– $\text{C}_3\text{H}_7(n)$ bond is a large degree of polarity in the bonding. In a recent study of metal–alkyl bond strengths for the transition metals of the entire second row it was shown that it is the ionic component of the binding that is responsible for the trends.³⁶ A major argument invoked was that the differences in bond strengths for different alkyls, like methyl, ethyl, isopropyl, and *n*-propyl, increase markedly to the left in the periodic table, where the bond polarity is larger due to the lower ionization potentials of these metals. For all metals the methyl bond strength is stronger than the ethyl bond strength which in turn is stronger than the isopropyl bond strength. The *n*-propyl bond strength is also significantly stronger than the isopropyl bond strength. These trends are explained by the size of the negative charge on carbon. The more methyl substituents there are on the carbon, the less negative is the charge on carbon and the weaker is the metal–carbon bond. The presence of the strongly electronegative chloride ligands in the present platinum complexes clearly leads to a substantially positively charged platinum atom even though the charge is very far away from the valence state of +2.

e. An Alternative Oxidative Addition/Reductive Elimination Sequence. An oxidative addition pathway has been suggested for the Shilov reaction in recent work by Stahl, Labinger, and Bercaw³⁷ who find that $[\text{Pt}(\text{en})(\text{CH}_2\text{Ph})\text{Cl}]$ undergoes oxidative addition of HCl at -78°C to give $[\text{HPt}(\text{en})(\text{CH}_2\text{Ph})\text{Cl}_2]$ (en = ethylenediamine). On warming, this Pt(IV) alkyl hydride loses a Cl^- ion to give a kinetically-inferred but unobserved intermediate that in turn rapidly loses toluene. Assuming the intermediate is an alkyl hydride, one can invoke reversibility arguments to make the case that C–H oxidative addition to Pt(II) may occur in the key step of the Shilov reaction. The intermediate might, however, undergo rearrangement to an agostic complex of the type $[\text{Pt}(\text{en})(\text{H}-\text{CH}_2\text{Ph})\text{Cl}]^+$, which would be compatible with the σ bond metathesis pathway.

We have therefore looked at the oxidative addition pathway in the model system. The corresponding Pt(IV) species, *cis,trans*- $[\text{Pt}(\text{H})\text{Me}(\text{OH}_2)_2\text{Cl}_2]$ (Figure 9), is indeed stable, being only 4.6 kcal/mol in energy above the outer-sphere methane

(34) Norman, R. O. C. *Principles of Organic Synthesis*; Chapman and Hall: London, 1978; p 85.

(35) McMillen, D. F.; Golden, D. M. *Annu. Rev. Phys. Chem.* **1982**, *33*, 493.

(36) Siegbahn, P. E. M. *J. Phys. Chem.* **1995**, *99*, 12723.

(37) Stahl, S. S.; Labinger, J. A.; Bercaw, J. E. *J. Am. Chem. Soc.* **1995**, *117*, 9371.

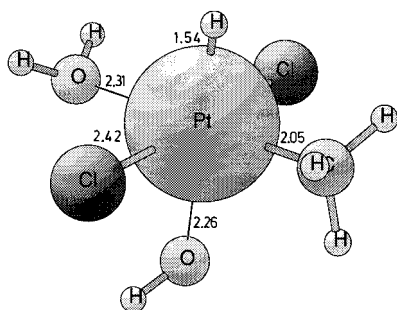


Figure 9. Structure of the $\text{PtCl}_2(\text{OH})_2\text{H}(\text{CH}_3)$ Pt(IV) complex, obtained after an oxidative addition reaction.

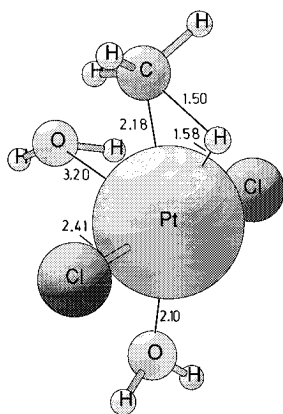


Figure 10. Structure of the $\text{PtCl}_2(\text{OH})_2\text{H}(\text{CH}_3)$ transition state for the oxidative addition reaction.

complex. The appropriate transition state for loss of OH_2 and reductive elimination, see Figure 10, is comparable in energy with the σ bond metathesis transition state. Without entropy effects this transition state is 23.8 kcal/mol above the outer sphere methane complex. The entropy effects calculated for this complex actually reduce the barrier further by 2.1 kcal/mol. However, the present model is inadequate for the calculation of entropy effects for this particular structure. As seen in Figure 10, one water molecule is almost free in this model which leads to a large entropy gain. In reality, this water molecule is engaged in hydrogen bonding with other solvent molecules. If this effect had been included in the computational model (which is too expensive in practice), it is likely that entropy effects actually would increase the barrier slightly instead. It should be added that this problem is only present for this particular structure in the present study. In all other structures, all ligands are bound in a way reasonably representative of the real situation. For the present purposes it is sufficient to conclude that the barrier should be somewhere above 23.8 kcal/mol, which is thus (just like the barrier for σ bond metathesis) in reasonable agreement with the measured barrier of about 28 kcal/mol. The PCI-80 calibration calculations show that this dissociation is well described at the B3LYP level. The calculated barriers for these two pathways are thus too close in energy for the case of the platinum reaction to distinguish these pathways. However, for Pd this transition state lies 36.0 kcal/mol above the outer sphere methane complex. The well-known instability of Pd(IV) makes the oxidative addition pathway completely implausible in this case.

f. Oxidative Addition or σ Bond Metathesis? σ bond metathesis pathways are very difficult to distinguish experimentally from oxidative addition/reductive elimination sequences, except for d^0 metals where oxidative addition is not permitted. The two pathways tend to have rather similar selectivity and rate dependence on the coligands. The similarity

of the two processes is perhaps not surprising when we consider that the transition state structures for the two cases are rather similar. The differences tend to manifest themselves after the transition state: in oxidative addition, the H ends up on the metal, but in σ bond metathesis it ends up on a *cis*-ligand.

For Pd(II) and especially Hg(II), a σ bond metathesis pathway must be involved, in view of the instability of Pd(IV) and the nonexistence of Hg(IV). Since Pt(II), Pd(II),⁸ and Hg(II)⁹ are the three best known catalysts for Shilov type chemistry, assigning a σ bond metathesis pathway to all three is therefore most economical and attractive in accounting for the strong similarities found. In the best-studied case of Pt(II), a number of features of the reaction are most consistent with σ bond metathesis. The rate of reaction is found to increase with decreasing IP of the alkane or arene very closely, and the fact that both types of substrate follow the same curve suggests the same mechanism is adopted for both.³⁸ Such a relationship is reasonable for a σ bond metathesis reaction but has never been found for the oxidative addition pathway. There is also a sharp fall off in activity by a factor of 100 on moving from $[\text{PtCl}_2(\text{OH})_2]$ to $[\text{PtCl}_3(\text{OH}_2)]^-$ and to $[\text{PtCl}_4]^{2-}$.^{1e} This would not be expected on the oxidative addition model, because the chloride ions should stabilize Pt(IV). Again in agreement with σ bond metathesis, hard base ligands for Pt give the highest reactivity.^{1f}

We conclude that Hg and Pd proceed by a σ bond metathesis mechanism and Pt may well also do the same, although an oxidative addition/reductive elimination sequence cannot be safely excluded in this case.

Conclusions

The results suggest that the Shilov reaction goes via transfer of a hydrogen atom from a methane σ complex, first to a neighboring Cl ligand in what is best described as a σ bond metathesis and then to solvent water. This avoids the formation of Pt(IV) and is quite similar to the mechanism proposed by Shilov himself. Methane has such a high $\text{p}K_a$ that a mechanism involving full deprotonation would be very endothermic, but the metal provides a route for net proton transfer to solvent in which both the incipient methyl group and the proton being transferred are strongly stabilized by coordination. At the transition state for the C–H activation the hydrogen atom being transferred is not very protonic, however. This is best seen in a calculation where an additional water is placed close to the transferred hydrogen. If the hydrogen atom would have been protonic, this would have led to a stabilization of the transition state. Instead, the added water molecule moved away from the C–H bond breaking region in the geometry optimization. The Mulliken charge on the hydrogen atom, which is a less certain measure of the protonic character, did not show any tendency of becoming very positive either. The charge is rather similar to the ones for the hydrogen atoms in methane.

An alternative oxidative addition/reductive elimination sequence was also investigated and was found to be competitive with the σ bond metathesis pathway for Pt, but is not tenable for Pd(II) or Hg(II). Although a σ bond metathesis mechanism seems more likely for Shilov chemistry with Pt, an oxidative addition/reductive elimination sequence cannot be safely excluded in the Pt case.

The breaking of a C–H bond in methane occurs in two steps. In the first step methane is coordinated to the metal. The energy requirement for this step is 10.5 kcal/mol for the best model used here. In the second step the C–H bond is broken with a

(38) Hodges, R. J.; Webster, D. E.; Wells, P. B. *J. Chem. Soc., Dalton Trans.* **1972**, 1972.

calculated barrier for the σ bond metathesis pathway of 16.5 kcal/mol. The total activation energy is thus the sum of these two energies which is 27 kcal/mol. This value is in very good agreement with the experimental estimate of 28 kcal/mol. To the calculated activation energy, zero-point vibrational and temperature effects contribute -2.9 kcal/mol, while long-range dielectric effects contribute -1.7 kcal/mol. For the oxidative addition pathway, a slightly lower barrier of 24 kcal/mol was obtained, but the entropy effects were left out in this case since they cannot be well predicted using the present model.

The second coordination sphere of the solvent plays an important role in the chemistry, not just as ultimate proton acceptor from the methane but also in the energetics of methane binding, an important factor because it directly contributes to the overall activation energy. The presence of only a few waters in the computational model allows these effects to be studied.

The origin of the unusual selectivity pattern for preferential attack on primary versus secondary CH bonds has been traced

to the higher bond strength in the *n*-alkyl versus the isoalkyl formed in the σ bond metathesis. By the Hammond postulate,³⁵ these bond strength differences are expected to lead to differences in the transition state energies for the two reactions. The bond strength differences are found to arise from differences in the polarity of the Pd-C bond in each case.

Quantum chemical calculations have in general tended to be more often applied in the past to structural rather than mechanistic problems, but the increasing power of the methods now available is beginning to change this picture. Experimental mechanistic studies have proved difficult in the Shilov system, and so it provides a case in which the value of such calculations is particularly clear.

Acknowledgment. R.H.C. thanks the NSF and P.E.M.S. thanks the NFR for funding.

JA9541894